Unconstrained Speech Segmentation using Deep Neural Networks

Van Zyl van Vuuren[1], Louis ten Bosch[2] and Thomas Niesler[1]
[1]*Department of Electrical and Electronic Engineering, University of Stellenbosch, Stellenbosch, South Africa*
[2]*Department of Linguistics, Radboud University, Nijmegen, The Netherlands*

Keywords: Unconstrained Automatic Speech Segmentation, Deep Neural Networks, Generative Pre-training.

Abstract: We propose a method for improving the unconstrained segmentation of speech into phoneme-like units using deep neural networks. The proposed approach is not dependent on acoustic models or forced alignment, but operates using the acoustic features directly. Previous solutions of this type were plagued by the tendency to hypothesise additional incorrect phoneme boundaries near the phoneme transitions. We show that the application of deep neural networks is able to reduce this over-segmentation substantially, and achieve improved segmentation accuracies. Furthermore, we find that generative pre-training offers an additional benefit.

1 INTRODUCTION

Speech can be segmented into phonemes manually by phonetic specialists, but this is known to be tedious, expensive and subjective. The use of accurate and reliable automatic segmentation algorithms is a desirable alternative. Especially when little or no transcribed phonetic material is available, such algorithms can facilitate the development of pronunciation dictionaries, and can be used to obtain suitable bootstrapping acoustic training data, thereby substantially accelerating the development of automatic speech recognition (ASR) systems. Automatic segmentation algorithms are also useful outside ASR, such as for the study of pronunciation variation, the development of coherent large-scale dictionaries, and in text-to-speech (TTS) applications (Sharma and Mammone, 1996; Wang et al., 2003; Adell et al., 2005).

A distinction can be made between segmentation approaches that require phone or orthographic transcripts, and those that do not. These two approaches are often referred to as **constrained** and **unconstrained** respectively (Keri and Prahallad, 2010).

Constrained speech segmentation algorithms are usually based on a forced alignment between phone-based hidden Markov models (HMMs) and the acoustic feature (Adell et al., 2005; Keri and Prahallad, 2010; Hoffmann and Pfister, 2010). In a severely under-resourced setting, it may not be possible to obtain suitable phone models. Indeed, the phone inventory itself may not yet be fully known.

Unconstrained speech segmentation algorithms detect segment boundaries using only the acoustic features. Because this approach does not require acoustic models, it can for example be applied in situations where the phone inventory has not yet been established. Popular past approaches to this problem are based on finding peaks in vector distance functions that respond to the dynamics of the acoustic features (Aversano et al., 2001; Sarkar and Sreenivas, 2005; Estevan et al., 2007; ten Bosch and Cranen, 2007; Räsänen et al., 2011). The focus of this paper is specifically on unconstrained speech segmentation.

Artificial neural networks (ANNs) have been applied to both constrained and unconstrained speech segmentation. In the former case, use is usually made of hybrid HMM/ANN systems in which multilayer perceptrons (MLPs) act either as phone probability estimators (Finster, 1992; Malfrere et al., 1998), or are used to detect phoneme transitions in order to refine the boundaries produced by an HMM alignment (Toledano, 2000; Lee, 2006). In the latter case, the ANN's are trained to estimate a **local score**, which is a value that indicates rapid changes in the features extracted from the audio signal, and therefore gives an indication of when a phoneme boundary is likely to be present (Suh and Lee, 1996; Keri and Prahallad, 2010). Maxima in the local score that are above a certain threshold are taken to correspond to a hypothesised segment boundary. This family of algorithms can deliver excellent performance but also suffers from the insertion of surplus boundaries (over-segmentation). These are due to clusters of maxima in the local score, not all of which correspond to true

Zyl van Vuuren V., ten Bosch L. and Niesler T..
Unconstrained Speech Segmentation using Deep Neural Networks.
DOI: 10.5220/0005201802480254
In *Proceedings of the International Conference on Pattern Recognition Applications and Methods* (ICPRAM-2015), pages 248-254
ISBN: 978-989-758-076-5

boundaries. Recently, we have addressed this by embedding an ANN local score estimator within a dynamic programming (DP) framework, and were able to show reduced over-segmentation and improved performance (van Vuuren et al., 2013). In the current paper we build on this work by employing deep neural network architectures as local score estimators.

The remainder of this paper is structured as follows. Sections 2 and 3 describe the application of deep belief networks to the unconstrained segmentation problem, Section 4 describes the way in which we assess the accuracy of competing systems, and Sections 5 and 6 respectively describe the experimental set-up and results. Finally, Section 7 concludes.

2 RESTRICTED BOLTZMANN MACHINES

Restricted Boltzmann machines (RBMs) have proved to be useful building blocks in the creation of deep neural architectures, and have recently achieved high accuracies in phone classification experiments (Mohamed et al., 2012). We hoped to emulate this success for the unconstrained speech segmentation task by using RBMs to achieve a more accurate local score.

An RBM is an energy-based stochastic generative model that can learn a probability distribution from observations by training the parameters of an undirected bipartite graph, also known as a Markov random field (MRF) (Fischer and Igel, 2012). The visible nodes $\mathbf{v} = (v_1, ..., v_m)$ and hidden nodes (latent variables) $\mathbf{h} = (h_1, ..., h_n)$ are illustrated in Figure 1, where each node represents a random variable.

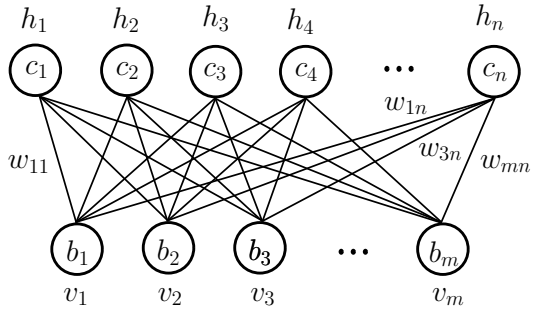

Figure 1: A restricted Boltzmann machine (RBM).

Each node has an associated real-valued bias indicated by b_i and c_j for the ith visible and jth hidden node respectively. Furthermore, each undirected connection (edge) between a visible node $v_i \in \{1, ..., m\}$ and hidden node $h_j \in \{1, ..., n\}$ has an associated real-valued weight w_{ij}. The joint probability distribution over visible and hidden nodes is the Boltzmann distribution (Bishop et al., 2006), and is given by Equation 1,

$$p(\mathbf{v}, \mathbf{h}) = \frac{1}{Z} e^{-E(\mathbf{v}, \mathbf{h})} \quad (1)$$

where Z is the partition function given by Equation 2.

$$Z = \sum_{\mathbf{v}, \mathbf{h}} e^{-E(\mathbf{v}, \mathbf{h})} \quad (2)$$

Associated with each configuration of values for the visible $\mathbf{v}$ and hidden $\mathbf{h}$ nodes of the RBM is a scalar value $E(\mathbf{v}, \mathbf{h})$ called the energy as given by Equation 3.

$$E(\mathbf{v}, \mathbf{h}) = -\sum_{i=1}^{m} \sum_{j=1}^{n} w_{ij} v_i h_j - \sum_{i=1}^{m} b_i v_i - \sum_{j=1}^{n} c_j h_j \quad (3)$$

Binary RBMs have binary stochastic nodes for which the visible and hidden nodes have associated binary values, i.e. $(\mathbf{v}, \mathbf{h}) \in \{0, 1\}^{m+n}$. Furthermore, the probability of a 1 being associated with a visible or hidden node, given the hidden or visible vectors respectively, can be shown to be a sigmoid function. To increase the probability of an observed or training vector the weights are adjusted by gradient ascent in order to maximise the log-likelihood of the training sample. Since this is exponentially computationally expensive, an approximate training procedure known as contrastive divergence (CD) is used instead of the exact maximum likelihood learning (Bengio, 2009; Krizhevsky and Hinton, 2009; Fischer and Igel, 2012). CD employs Gibbs sampling to sample from the model's distribution. The resulting weight update is given by Equation 4, where ε is the learning rate and $\mathbf{v}^k$ is the k_{th} Gibbs sample. The update equation for the biases is similar.

$$\Delta w_{ij} = \varepsilon(p(h_j = 1|\mathbf{v}^0)v_i^0 - p(h_j = 1|\mathbf{v}^k)v_i^k) \quad (4)$$

In the literature it is common to use 1 step CD (Erhan et al., 2010), and this approach was followed in our experiments.

Because the input will be real-valued, the visible nodes of the RBM at the bottom of the stack of RBMs will be modelled as Gaussian instead of binary. An RBM with Gaussian visible nodes and binary hidden nodes is referred to as a Gaussian-Bernoulli RBM (GBRBM), and has the energy function shown in Equation 5 (Krizhevsky and Hinton, 2009), where σ_i is the standard deviation of the i_{th} visible Gaussian variable.

$$\begin{aligned} E(\mathbf{v}, \mathbf{h}) &= \sum_{i=1}^{m} \frac{(v_i - b_i)^2}{2\sigma_i^2} - \sum_{j=1}^{n} c_j h_j \\ &\quad - \sum_{i=1}^{m} \sum_{j=1}^{n} \frac{v_i}{\sigma_i} h_j w_{ij} \end{aligned} \quad (5)$$

To simplify learning, some authors (Cho et al., 2011) advise the use of a fixed variance, commonly $\sigma_i = 1$. The conditional probability for the visible nodes given the hidden nodes is then given by Equation 6,

$$p(v_i = v|\mathbf{h}) = \mathcal{N}\left(v \middle| b_i + \sigma_i \sum_j h_j w_{ij}, 1\right) \quad (6)$$

where $\mathcal{N}(\cdot|\mu,\sigma^2)$ is a Gaussian distribution with mean μ and variance σ^2. Another simplification is to use the means (μ_i) of the visible nodes (Equation 6) as the samples instead of sampling from the Gaussian distribution during Gibbs sampling. This is done because the standard deviations are not updated and therefore samples from the Gaussian distribution will be either dominated by noise or are only slightly affected by the standard deviation. These restrictions were applied in the experiments that follow, and therefore all the features in the training data were preprocessed to have zero mean and unit variance before training the GBRBM. In this way the contrastive divergence algorithm can remain unchanged.

3 PRE-TRAINING OF DEEP NETWORKS

To generatively pre-train a deep network, RBMs are stacked in layers. The first RBM is a GBRBM trained to generate the input data. After this, the probability of activation for the hidden nodes, generated from the training data, is used as the training data for next RBM layer. This procedure is known as greedy layer-wise learning (Hinton et al., 2006; Bengio et al., 2007). As the RBMs are stacked, more abstract features are detected by the higher RBMs. Finally a layer of neurons corresponding to the labels of the classification problem is added to the top of the the network. The parameters of the network can then be fine-tuned by backpropagation. We will conduct experiments both with and without generative pre-training of the networks in order to establish its benefits for the unconstrained speech segmentation task.

4 ASSESSMENT OF SEGMENTATION ACCURACY

The *R*-value is a scalar value between 0 and 1 that has been proposed for the assessment of segmentation accuracy (Räsänen et al., 2009). Equations 7 and 8 define two quantities known as the hit rate (*HR*) and over-segmentation (*OS*) respectively in terms of the number of hits (N_{hit}), the number of hypothesised boundaries (N_f), and the number of reference boundaries (N_{ref}) in an utterance. The number of hits is the number of hypothesised boundaries within 20ms of a true boundary.

$$HR = \frac{N_{hit}}{N_{ref}} \quad (7)$$

$$OS = \frac{N_f}{N_{ref}} - 1 \quad (8)$$

The *R*-value is defined as the average of two distances r_1 and r_2 which are themselves defined on a plane whose axes are *HR* and *OS*. The distances r_1 and r_2 are determined by using Equations 9 and 10 respectively, and subsequently the *R*-value by Equation 11.

$$r_1 = \sqrt{(1-HR)^2 + OS^2} \quad (9)$$

$$r_2 = \frac{-OS + HR - 1}{\sqrt{2}} \quad (10)$$

$$R = 1 - \frac{abs(r_1) + abs(r_2)}{2} \quad (11)$$

The larger r_1 or r_2, the smaller the *R*-value will become. Hence, the larger the *R*-value, the better the segmentation performance. Informal testing revealed that when the number of hypothesised boundaries becomes substantially more than the number of true phoneme boundaries, it is likely that the neural network is overfitting. The *R*-value strongly penalises over-segmentation, and is therefore effective at combating overfitting when using early stopping during training, as described later in Section 5.3. Other performance measures found in the literature do not explicitly penalise over-segmentation.

5 EXPERIMENTAL SET-UP

5.1 Data

Our experimental evaluations are based on the TIMIT database (Fisher et al., 1986), which has also been employed by several other authors for the evaluation of unconstrained speech segmentation algorithms (Aversano et al., 2001; Sarkar and Sreenivas, 2005; Estevan et al., 2007; Keri and Prahallad, 2010; Räsänen et al., 2011). The TIMIT data offers a phonetic segmentation (i.e. the locations of phone boundaries) that has been produced by human phonetic experts. Such a carefully prepared manual segmentation is not found in other, more recent, speech databases.

The standard TIMIT 462-speaker training set will be used to train the segmentation algorithms. The development set consists of 50 speakers drawn from the full 168-speaker test set, and is used to optimise high-level parameters of the algorithms (Halberstadt, 1998). The standard TIMIT 24-speaker core test set is used exclusively for final testing. There is no speaker overlap between any of these three sets.

In all experiments, a frame length of 10ms with a frame skip of 5ms was used during feature extraction. Each frame of speech was represented by a 39-dimensional feature vector consisting of 12 MFCCs, log energy, and appended first and second derivatives.

5.2 Baseline Systems

For purposes of comparison, two unconstrained segmentation systems were included as baselines for our proposed approach. These baseline systems have been described previously by (Keri and Prahallad, 2010) and by (van Vuuren et al., 2013).

5.2.1 MLP-based Segmentation

A multi-layer perceptron (MLP) can be used to compute a local score on the basis of a group of consecutive feature vectors by training an output neuron to produce a 1 when the evidence in the input feature vectors supports the presence of a boundary, and a value of 0 when the evidence supports the absence of a boundary. This approach has been shown by (Keri and Prahallad, 2010) to lead to state-of-the-art performance. This system has therefore been included as a baseline for our experiments.

A segment boundary is hypothesised at the frame at which the local score is at a maximum within a search region, as demonstrated by Equation 12.

$$[\hat{B_R}] = \underset{t \in \{S_R \ldots E_R\}}{\operatorname{argmax}} \{LS(i_t)\} \qquad (12)$$

Here i_t is the i_{th} frame, S_R and E_R are the start and end of the search region respectively, $LS(i_t)$ is the local score at frame i_t, and B_R is the hypothesised segment boundary. The search region is defined as an interval within which the local score exceeds a value of 0.5.

As proposed by (Keri and Prahallad, 2010), our baseline MLP-based segmentation system used a network with single hidden layer and 30 hidden neurons. Training data consisted of feature vector groups located around phoneme boundaries in the TIMIT training set and feature vector groups midway between two boundaries. The network was trained using back-propagation without pre-training, with groups of 11 feature vectors centred about the point of interest.

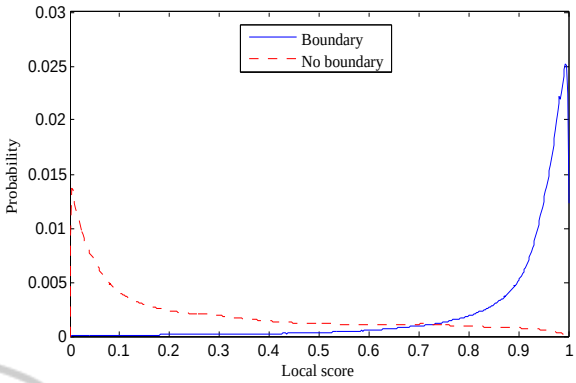

Figure 2: Probability distribution of MLP-based local score values at, and away from, phoneme boundaries, estimated from TIMIT.

Figure 2 shows the distribution of the local score values computed on the TIMIT corpus by the resulting MLP. The limited overlap of these two distributions indicates that the local score can achieve good discrimination between locations at which a boundary is present, and location where it is not.

5.2.2 Dynamic Programming

The local score can be embedded in a dynamic programming (DP) framework that includes an explicit probabilistic model for the length of a segment. The segmentation of a speech utterance is then formulated as a Markov model, where each frame corresponds to a state. The transition probabilities correspond to the probability of the corresponding hypothesised segment length, as established from a corpus such as TIMIT and shown in Figure 3. The Markov emission probabilities are calculated from the distribution of the local score values $LS(i_t)$, which were shown in Figure 2.

Using these distributions, the probability of a boundary given the local score at a particular frame can be calculated and this serves as the basis of the DP search. We have shown recently that this embedding of a MLP-based local score in a DP framework can reduce the insertion incorrect boundaries when the local score exhibits multiple closely-spaced maxima (van Vuuren et al., 2013). We have therefore included such a system as a second baseline for our experiments.

5.3 RBM-based Systems

All RBM-based systems used in our experiments have logistic sigmoid neurons, since sigmoid functions are also used to sample values from an RBM. We will consider networks with between 1 and 5 hidden layers, with each hidden layer having the same number

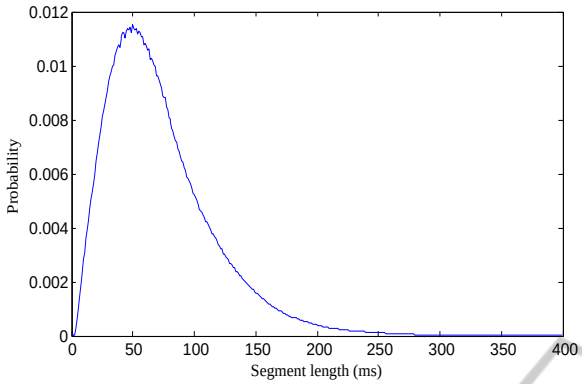

Figure 3: Probability distribution of phoneme lengths in the TIMIT training set.

of neurons (256, 512 or 1024). For each network architecture, a network is prepared with and without pre-training. The subsequent supervised training by backpropagation employs early stopping to find the best performing network on the development set, after which the network's performance was tested on the TIMIT core test set.

Early stopping is a technique used to avoid overfitting during supervised training of neural networks (Erhan et al., 2010). After each training epoch the network's development set performance is compared to the previous epoch's performance. When the performance deteriorates, the learning rate is halved. Training then continues from the previous epoch's weight values. We found that the networks's performance tends to alternate slightly between epochs, although improving in the longer term. For this reason we chose to halve the learning rate only when the performance drops consistently over 5 trial epochs.

For generative pre-training each RBM was subjected to 50 training epochs, i.e. 50 epochs of unsupervised training per layer of the DBN, at a learning rate of 0.005 for the Gaussian Bernoulli RBM and 0.05 for the binary RBMs, and with a momentum of 0.9. These values were chosen to be similar to those used to train RBM-based acoustic models for phone classification (Mohamed et al., 2012). Early stop training starts with a learning rate of 0.1 and momentum of 0.9, and continues until the learning rate is smaller than 0.01. Stochastic gradient descent and unsupervised pre-training used mini-batches consisting of 128 training samples.

An input vector to the neural network consisted of the features associated with 11 consecutive frames centred on the test frame. Since the feature vector extracted from each frame was 39-dimensional, each input vector had a total of 429 components.

6 EXPERIMENTAL RESULTS

Every network architecture was subjected to three early stop training sessions, from which a mean performance was calculated. This average is taken to indicate typical performance. Figure 4 shows this performance on the TIMIT core test set for 256, 512, and 1024 hidden neurons per hidden layer.

When the number of hidden layers is increased from 1 to 2, there is in all cases a notable performance improvement. However, when 3 or more hidden layers are used, further gains are not reliably achieved. There is gradual improvement in performance as the number of neurons per hidden layer is increased.

The core test set performance of the networks with best performance on the development set, with and without pre-training are shown in Table 1. The networks with and without pre-training contained 5 and 3 hidden layers respectively, both with 1024 neurons per layer (Figure 4). The performance of the pre-trained network when embedded in the DP algorithm as described in Section 5.2.2 is also shown.

Hypothesised boundaries falling outside a 20ms region around the true phoneme boundaries are regarded as insertions, and missed phoneme boundaries as deletions. The average percentage insertions and deletions per reference phoneme boundary are included in the table. Both deep networks achieve substantial improvements in segmentation performance. Best performance is achieved when pre-training is applied. It is interesting to see that the incorporation of dynamic programming leads to deteriorated performance in our DNN experiments. Since the chief motivation for the dynamic programming framework was to reduce over-segmentation, this indicates that the local scores estimated by the deep networks are less prone to these insertion errors, and therefore the incorporation of DP is unnecessary and even counterproductive.

7 DISCUSSION AND CONCLUSION

Our experiments show that a deep neural network is able to provide a substantially better local score for use in unconstrained speech segmentation than previously proposed alternatives. Pre-training provides a performance benefit, as does a larger number of neurons per hidden layer. Furthermore, the local scores estimated by deep networks appear to reduce the tendency to over-segment that has been associated with this class of algorithms in the past. Other means of reducing over-segmentation, such as the introduction of

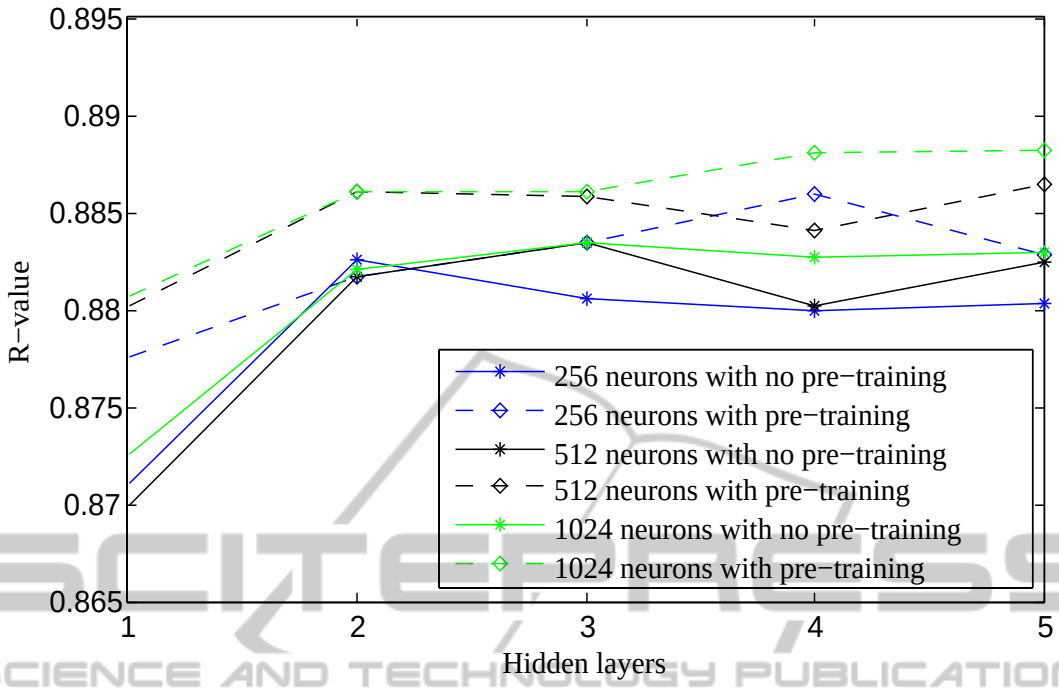

Figure 4: Segmentation performance on the TIMIT core test set for networks with 256, 512, and 1024 hidden neurons per layer, and with between 1 and 5 hidden layers.

Table 1: Comparison of segmentation performance, measured on the TIMIT core test set, of systems with best performance on the development set.

System	Ins(%)	Del(%)	R-value
MLP benchmark from (Keri and Prahallad, 2010)	12.74	17.00	0.857
MLP with DP benchmark from (van Vuuren et al., 2013)	13.06	15.72	0.863
DNN without pre-training	11.17	12.73	0.887
DNN with pre-training	10.14	12.66	0.891
DNN with DP and pre-training	13.12	14.05	0.868

probabilistic models for segment length and dynamic programming, therefore no longer lead to any performance benefit. This simplifies the segmentation algorithm.

In the future we plan to investigate whether the performance benefit of our proposed algorithm persists when applied to data substantially different from the TIMIT training material. We are particularly interested to know the behaviour of unconstrained segmentation algorithms trained on TIMIT but applied to entirely different languages. Eventually, we would like to determine whether such cross-domain segmentation can be used to facilitate the development of ASR systems for under-resourced languages.

ACKNOWLEDGEMENTS

This research was supported by the National Research Foundation of South Africa under grant UID 71926. Opinions expressed and conclusions arrived at are those of the authors and are not necessarily to be attributed to the NRF.

REFERENCES

Adell, J., Bonafonte, A., Gomez, J., and Castro, M. (2005). Comparative study of automatic phone segmentation methods for TTS. In *Proceedings of the IEEE International Conference on Acoustics, Speech, and Signal Processing (ICASSP)*.

Aversano, G., Esposito, A., Esposito, A., and Marinaro, M. (2001). A new text-independent method for phoneme

segmentation. In *Proceedings of the 44th IEEE Midwest Symposium on Circuits and Systems*.

Bengio, Y. (2009). Learning deep architectures for AI. *Foundations and Trends in Machine Learning*, 2(1):1–127.

Bengio, Y., Lamblin, P., Popovici, D., and Larochelle, H. (2007). Greedy layer-wise training of deep networks. *Advances in neural information processing systems*, 19:153.

Bishop, C. M. et al. (2006). *Pattern recognition and machine learning*, volume 1. Springer.

Cho, K. et al. (2011). Improved learning algorithms for restricted Boltzmann machines. Master's thesis, School of science, Aalto University.

Erhan, D., Bengio, Y., Courville, A., Manzagol, P.-A., Vincent, P., and Bengio, S. (2010). Why does unsupervised pre-training help deep learning? *The Journal of Machine Learning Research*, 11:625–660.

Estevan, Y. P., Wan, V., and Scharenborg, O. (2007). Finding maximum margin segments in speech. In *Proceedings of the IEEE International Conference on Acoustics, Speech, and Signal Processing (ICASSP)*.

Finster, H. (1992). Automatic speech segmentation using neural network and phonetic transcription. In *Proceedings of the International Joint Conference on Neural Networks (IJCNN)*.

Fischer, A. and Igel, C. (2012). An introduction to restricted Boltzmann machines. In *Progress in Pattern Recognition, Image Analysis, Computer Vision, and Applications*, pages 14–36. Springer.

Fisher, W. M., Doddington, G. R., and Goudie-Marshall, K. M. (1986). The DARPA speech recognition research database: specifications and status. In *Proceedings of the DARPA Workshop on Speech Recognition*.

Halberstadt, A. K. (1998). *Heterogeneous Acoustic Measurements and Multiple Classifiers for Speech Recognition*. PhD thesis, Massachusetts Institute of Technology, MIT.

Hinton, G. E., Osindero, S., and Teh, Y.-W. (2006). A fast learning algorithm for deep belief nets. *Neural computation*, 18(7):1527–1554.

Hoffmann, S. and Pfister, B. (2010). Fully automatic segmentation for prosodic speech corpora. In *Proceedings of Interspeech*.

Keri, V. and Prahallad, K. (2010). A comparative study of constrained and unconstrained approaches for segmentation of speech signal. In *Proceedings of the International Conference on Spoken Language Processing (ICSLP)*.

Krizhevsky, A. and Hinton, G. (2009). Learning multiple layers of features from tiny images. Master's thesis, Department of Computer Science, University of Toronto.

Lee, K.-S. (2006). MLP-based phone boundary refining for a TTS database. *IEEE Transactions on Audio, Speech and Language Processing*, 14(3):981–989.

Malfrere, F., Deroo, O., and Dutoit, T. (1998). Phonetic alignment : Speech synthesis based vs. hybrid HMM/ANN. In *Proceedings of the International Conference on Spoken Language Processing (ICSLP)*.

Mohamed, A.-r., Dahl, G. E., and Hinton, G. (2012). Acoustic modeling using deep belief networks. *IEEE Transactions on Audio, Speech, and Language Processing*, 20(1):14–22.

Räsänen, O., Laine, U., and Altosaar, T. (2011). Blind segmentation of speech using non-linear filtering methods. *Speech Technologies*, pages 105–124.

Räsänen, O. J., Laine, U. K., and Altosaar, T. (2009). An improved speech segmentation quality measure: the R-value. In *Proceedings of Interspeech)*.

Sarkar, A. and Sreenivas, T. (2005). Automatic speech segmentation using average level crossing rate information. In *Proceedings of the IEEE International Conference on Acoustics, Speech, and Signal Processing (ICASSP)*.

Sharma, M. and Mammone, R. (1996). 'Blind' speech segmentation: automatic segmentation of speech without linguistic knowledge. In *Proceedings of the Fourth International Conference on Spoken Language Processing (ICSLP)*.

Suh, Y. and Lee, Y. (1996). Phoneme segmentation of continuous speech using multi-layer perceptron. In *Proceedings of the Fourth International Conference on Spoken Language (ICSLP)*.

ten Bosch, L. and Cranen, B. (2007). A computational model for unsupervised word discovery. In *Proceedings of Interspeech*.

Toledano, D. (2000). Neural network boundary refining for automatic speech segmentation. In *Proceedings of the IEEE International Conference on Acoustics, Speech, and Signal Processing (ICASSP)*.

van Vuuren, V. Z., ten Bosch, L., and Niesler, T. (2013). A dynamic programming framework for neural network-based automatic speech segmentation. In *Proceedings of Interspeech*.

Wang, D., Lu, L., and Zhang, H.-J. (2003). Speech segmentation without speech recognition. In *Proceedings of theInternational Conference on Multimedia and Expo, ICME*.